

# Pharmacokinetic Characteristics of Capsaicin-Loaded Nanoemulsions Fabricated with Alginate and Chitosan

Ah Young Choi,<sup>‡</sup> Chong-Tai Kim,<sup>§</sup> Hee Yoon Park,<sup>‡</sup> Han Oll Kim,<sup>‡</sup> Na Ra Lee,<sup>‡</sup> Kyung Eun Lee,<sup>‡</sup> and Hye Sun Gwak<sup>\*‡</sup>

<sup>‡</sup>College of Pharmacy and Division of Life and Pharmaceutical Sciences, Ewha Womans University, 52 Ewhayeodae-gil Seodaemun-gu, Seoul 120-750, Korea

<sup>§</sup>Bio-Nano Research Center, Korea Food Institute, Seongnam, Gyeonggi 463-746, Korea

**ABSTRACT:** Nanotechnologies are being employed to enhance the stability and oral bioavailability of lipophilic substances, such as capsaicin. This study aimed to examine the pharmacokinetic properties of the formulated capsaicin-loaded nanoemulsions. A pharmacokinetic study was carried out using double-layer nanoemulsions fabricated with alginate and chitosan polymers and triple-layer nanoemulsions fabricated with chitosan/alginate polymers. Capsaicin nanoemulsions and capsaicin control (oleoresin capsicum) were administered to the rat at a dose of 10 mg/kg. A statistically significant difference was found in the area under the curve from time zero to time infinity ( $AUC_{inf}$ ) among formulations ( $p < 0.01$ ). In comparison to the control group, the relative bioavailability of formulated nanoemulsions was up to 131.7. The  $AUC_{inf}$  increased in a nano-size-dependent manner; as nano size decreased,  $AUC_{inf}$  increased. IN comparison to the double-layer nanoemulsions, the triple-layer nanoemulsion showed a significantly increased volume of distribution, resulting in the increased clearance and decreased  $AUC_{inf}$ . It was concluded that the formulated nanoemulsions could significantly enhance the bioavailability of capsaicin.

**KEYWORDS:** Nanoemulsions, capsaicin, pharmacokinetic, bioavailability, polymers

## 1. INTRODUCTION

Capsaicin, the active component of chili peppers, is the major flavoring compound that gives food hot sensations. Capsaicin (*trans*-8-methyl-*N*-vanillyl-6-nonenamide) is a crystalline, colorless, and lipophilic alkaloid with a molecular weight of 305.40.<sup>1</sup>

Capsaicin topical treatment has been widely applied to treat pain. Capsaicin is known to bind to transient receptor potential vanilloid 1 (TRPV1), which is mainly expressed in the sensory neurons.<sup>2</sup> This receptor is a non-selective, ligand-operated cationic channel located primarily in the small fibers of nociceptive neurons.<sup>3</sup> Binding capsaicin to TRPV1 increases intracellular calcium, which triggers the release of the substance P and calcium gene-related peptides. Capsaicin transdermal delivery systems promote the desensitization of the sensory neuron caused by substance P depletion.<sup>4</sup>

Recently, the use of capsaicin was extended to other medical areas, such as cancer, cardiovascular diseases, and gastrointestinal disorders.<sup>5</sup> The anticancer effects were attributed to the ability of capsaicin to prevent cell proliferation and migration and induce cell apoptosis.<sup>6,7</sup> The cardiovascular benefits from capsaicin could result from its role in regulating cardiovascular functions through the release of neurotransmitters, such as calcitonin gene-related peptides and substance P. In addition, it was studied that capsaicin has effects of platelet aggregation inhibition and antioxidant, which would be beneficial against cardiovascular diseases. Low doses of capsaicin are known to increase the basal gastric mucosal blood flow and gastric mucus secretion and facilitate gastric epithelial restitution, resulting in the maintenance of gastrointestinal mucosa integrity against any injuries.<sup>8,9</sup>

As mentioned above, capsaicin is important in the food and pharmaceutical industries. However, its formulation to enhance

health conditions or prevent medical problems has been limited because of its low solubility in water and poor stability.

Nanotechnology, such as nanoemulsion delivery systems, is being employed to enhance the stability and oral bioavailability of lipophilic substances.<sup>10,11</sup> In addition, recent studies showed that the effects of capsaicin could be prolonged by controlling the release of capsaicin, using nanoparticles.<sup>12,13</sup> Thus far, most studies mainly focused on the physicochemical characteristics, stability, and *in vitro* study of nanoparticles; however, the *in vivo* evaluations of capsaicin nanoemulsion delivery systems are still lacking.

In our previous study, we successfully formulated double- and triple-layer nanoemulsions fabricated with natural biopolymers, such as alginate and chitosan, and characterized their structures and stabilities. The formulated nanoemulsions ranged from 50 to 150 nm, which were expected to enhance bioavailability.<sup>14,15</sup> Therefore, in this study, we aimed to examine the *in vivo* pharmacokinetic (PK) properties of the formulated capsaicin-loaded nanoemulsions using rats for the further development of capsaicin-containing food products.

## 2. MATERIALS AND METHODS

**2.1. Materials.** Oleoresin capsicum (OC, SHU 100 000) was supplied by G&F (Seoul, Korea). Chitosan was prepared by demineralization, deproteinization, and deacetylation from crab shell. Then, the chitosan (degree of deacetylation of 93% and molecular weight of 330 000) was dissolved in a mixed aqueous solution of 20%

**Received:** December 12, 2012

**Revised:** February 14, 2013

**Accepted:** February 15, 2013

**Published:** February 15, 2013

hydrochloride solution and distilled water, after which the mixture was adjusted to pH 5.6 and stirred for 3 h. The reaction mixture was subjected to a continuous membrane filtration process, and a permeate was freeze-dried.<sup>16</sup> Alginate sodium salt (from brown algae, ~3500 cP, 2%, 25 °C), verapamil hydrochloride [internal standard (IS)], and polyethylene sorbitan monooleate (Tween 80) were purchased from Sigma Chemical Co. (St. Louis, MO).

**2.2. Preparation of Chitosan-/Alginate-Based Nanoemulsions.** The self-assembly method<sup>14</sup> was employed to prepare double-layer nanoemulsions fabricated with alginate and chitosan polymers and a triple-layer nanoemulsion with chitosan/alginate polymers.

The alginate-/chitosan-based nanoemulsions were prepared using Tween 80, and various ratios of the OC and Tween 80 were used to obtain desirable sizes of nanoemulsions. The alginate and chitosan solutions were prepared at a concentration of 0.05% in aqueous phase under constant stirring, and the polymer solutions were then heated to 100 °C for 5 min with a heating and stirring plate and cooled to room temperature. To prepare the double-layer nanoemulsions of alginate and chitosan, 100 mL of 0.05% alginate and chitosan solutions was gradually added to 0.5 g of OC/Tween 80 with constant stirring using a laboratory mixer for 2 h at 25 °C, respectively. Alginate-/chitosan-based nanoemulsions were stabilized at 25 °C for 24 h and then filtered using a 0.45 μm polyvinylidene fluoride (PVDF) membrane filter (Whatman, U.K.).

To prepare the triple-layer nanoemulsions, the pH values of the 0.05% alginate and chitosan solutions were initially set to 4.9 and 4.6, respectively. The optimal formulation of the oil phase–surfactant mixture (0.75 g) was added to 117.5 mL of the 0.05% alginate solution and gently mixed for 30 min. To produce an alginate pre-gel, 7.5 mL of an 18 mM calcium chloride solution was added dropwise for 60 min under gentle stirring. Then, 25 mL of the 0.05% chitosan solution was added dropwise into the pre-gel over 90 min. A colloidal dispersion at pH 4.7 formed upon polycationic chitosan addition. The alginate-/chitosan-based nanoemulsion was stirred for 30 min to improve curing. The supernatant was collected by centrifugation and filtered with a 0.45 μm PVDF membrane filter.

**2.3. Characterization of Capsaicin-Loaded Nanoemulsions.**

**2.3.1. Determination of the Particle Size.** The particle size of the nanoemulsion was determined by a photon correlation spectroscopy, which analyzes the fluctuations in light scattering because of the Brownian motion of the particles, using a Nanotrak 250 (Microtrac, Inc., Montgomeryville, PA). Light scattering was monitored at 25 °C and an angle of 90°.

**2.3.2. Determination of the ζ Potential.** The ζ potential of nanoemulsion preparations was determined by placing 1 mL of the sample in a disposable ζ cuvette (1 × 1 × 4 cm). The cuvette was inserted into the measurement chamber of the particle electrophoresis instrument (Zetasizer Nanoseries ZS, Malvern Instrument, Worcestershire, U.K.) and equilibrated to 25 °C in the Peltier-controlled cuvette holder 2 min before use. The ζ potential was then determined by measuring the direction and velocity that the biopolymer nanoemulsion moved in the applied electric field at 633 nm for 1 min.

**2.3.3. Determination of Encapsulation Efficiency.** Capsaicin was extracted with 15 mL of a mixture of ethanol, acetone, and petroleum ether (1:1:4, v/v/v) from the nanoemulsion. The extracted solution was concentrated under vacuum and dissolved with isopropanol. The dissolved solution was measured by a high-performance liquid chromatography (HPLC) system consisting of a pump (Gradient Controller 601, Ever Seiko Corporation, Tokyo, Japan), a UV/vis detector (S-3740, Soma Optics, Ltd., Tokyo, Japan), and a data station (MultiChro, Yullin Technology, Seoul, Korea). Separation was performed on a C18 column (Zorbax Eclipse XDBC18, 4 × 6 × 250 mm, 5 μm, Agilent Technologies, Santa Clara, CA) with a gradient system. The mobile phase was a mixture of methanol and deionized water at a ratio of 70:30 (v/v). The flow rate was 0.8 mL/min for 30 min, and the UV/vis detector was set at 280 nm. The encapsulation efficiency was calculated using the following formula:

encapsulation efficiency (%)

$$= \left( \frac{\text{total amount of drug in the nanoemulsion}}{\text{total quantity of drug added initially during preparation}} \right) \times 100$$

**2.4. Validation of Blood Capsaicin Concentration Assay.**

**2.4.1. Preparation of Standard Solutions.** Working stock solutions of capsaicin (as an OC) and IS were prepared in methanol at a concentration of 1 mg/mL. Prior to use, these two stock solutions were further diluted with methanol to obtain working solutions at a concentration of 10 μg/mL, and an appropriate dilution of the working solution with drug-free plasma gave a concentration range between 0.5 and 50 ng/mL of capsaicin.

Six samples (0.5, 1, 5, 10, 25, and 50 ng/mL) for the calibration and quality control were prepared by spiking blank plasma with appropriate volumes of the working solutions.

**2.4.2. Sample Preparation.** All plasma samples were stored at –70 °C, thawed at room temperature, and vortex-mixed at 4 °C prior to analysis. Plasma samples (72 μL) were mixed with 8 μL of IS (100 ng/mL) solution, and 400 μL of acetonitrile was added to precipitate protein. The mixture was vortex-mixed for 5 min and centrifuged at 13 000 rpm for 10 min, and then the supernatant (5 μL) was injected directly into the HPLC system.

**2.4.3. Chromatographic Conditions.** The liquid chromatography (LC) system consisting of a triple quadrupole mass spectrometer (6460, Agilent Technologies, Santa Clara, CA) coupled with HPLC (1200, Agilent Technologies, Santa Clara, CA). The analytical column was a Zorbax X DB C18 (1.8 μm, 50 × 4.6 mm, Agilent Technologies, Santa Clara, CA). The isocratic mobile phase, a mixture of 5 mM ammonium formate and acetonitrile with 0.1% formic acid (20:80, v/v), was delivered at 0.4 mL/min. The mass spectrometer was equipped with an electrospray ionization source and operated in the selected reaction monitoring mode for precursor–product ion transitions for capsaicin ( $m/z$  306 → 137) and IS ( $m/z$  455 → 165). The optimum conditions for the analysis of the analytes were as follows: gas temperature, 350 °C; gas flow, 9 L/min; nebulizer pressure, 35 psi; sheath gas temperature, 400 °C; sheath gas flow, 10 L/min; capillary voltage, 4000 V; and nozzle voltage, 1500 V.

**2.4.4. Method Validation.** **2.4.4.1. Specificity.** The degree of interference by endogenous plasma constituents with capsaicin and IS was evaluated by inspection of the chromatogram derived from processed blank and spiked plasma samples and also from processed blank samples injected during each analytical run.

**2.4.4.2. Calibration Curve.** Calibration standards at concentrations of 0.5, 1, 5, 10, 25, and 50 ng/mL were extracted and assayed, as mentioned above. The calibration curve was constructed on the basis of the peak area ratio of capsaicin and IS.

**2.4.4.3. Accuracy and Precision.** The intraday accuracy and precision of the method were estimated by assaying five replicate plasma samples at six different concentrations, in five analytical runs. The overall mean precision was defined by the percentage of relative standard deviation (RSD) of five standards at six different concentrations analyzed on the same day. The interday accuracy and precision were estimated from the analysis of the six standards on 5 separate days during the method validation.

**2.5. PK Study.** **2.5.1. Animal Study.** All animal experiments adhered to the Principles for Biomedical Research Involving Animals developed by the Council for International Organizations of Medical Sciences. Male Sprague–Dawley rats weighing 250–300 g were obtained from Samtako Bio Co., Ltd. (Osan, Korea). The rats were anesthetized with ether (Daejung Chemicals and Metals, Siheung, Korea), and the jugular vein was cannulated using a polyethylene tube (0.76 mm inner diameter × 1.22 mm outer diameter; Becton Dickinson, Franklin Lakes, NJ). After surgery, each animal was housed in a separate cage. The animals fasted overnight, and the fasting continued for the first 6 h of the experiment; however, they were allowed water *ad libitum*. The rats were then divided into six groups, and each group was comprised of 6 rats. Groups 1–6 were orally administered with capsaicin control, three sizes (50, 100, and 150 nm) of nanoemulsions fabricated with alginate polymers (ANS0, AN100,

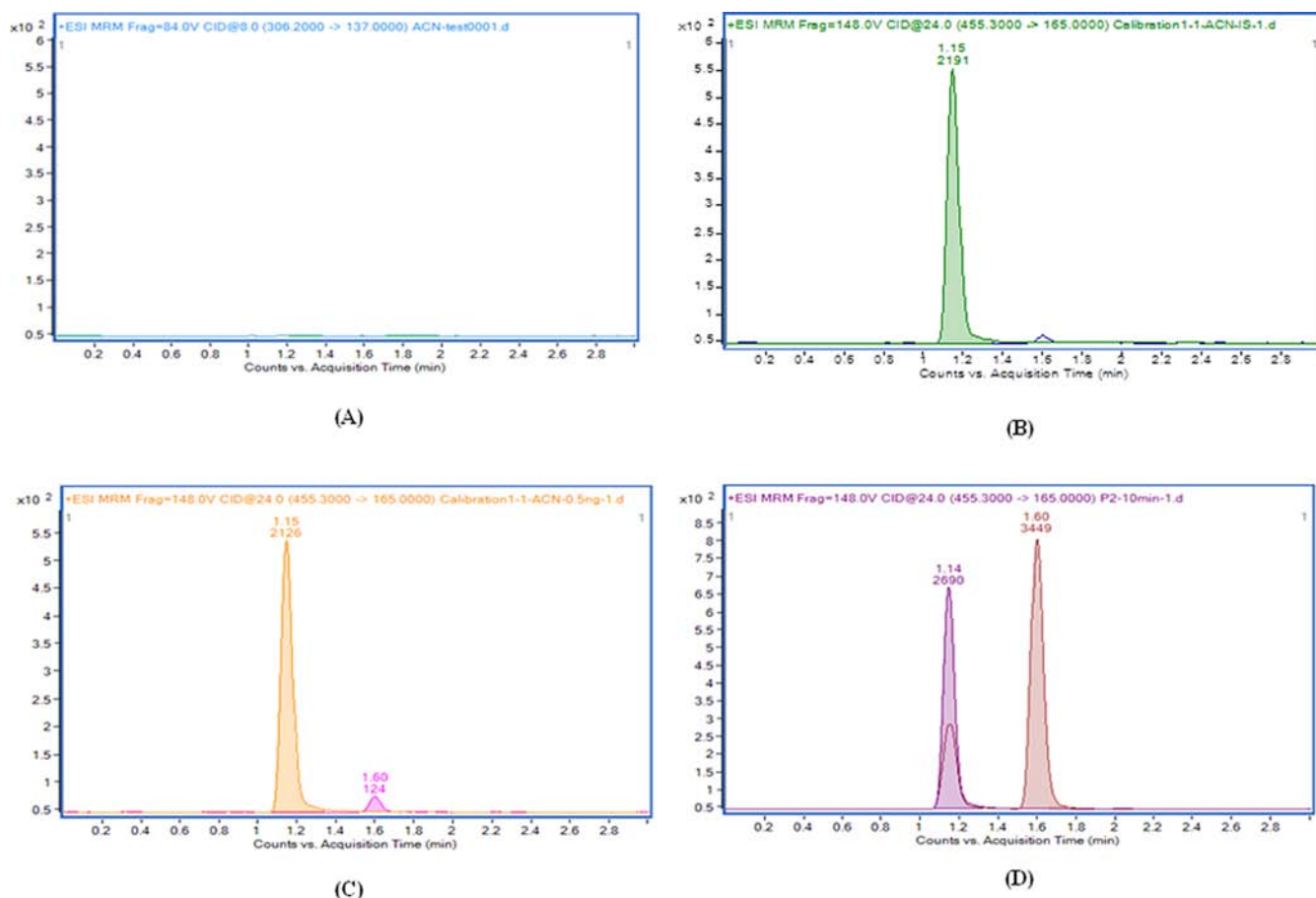


**Figure 1.** Chromatograms for (A) control rat plasma, (B) control plasma spiked with IS (10 ng/mL verapamil hydrochloride), (C) control plasma spiked with capsaicin (0.5 ng/mL as an OC) and IS (10 ng/mL), and (D) sample obtained from a rat at 10 min after oral administration of a double-layer nanoemulsion fabricated with alginate and chitosan (10 mg/kg as an OC).

AN150, respectively), and 100 nm nanoemulsions fabricated with chitosan (CN100) and chitosan/alginate (CAN100) polymers at a dose of 10 mg/kg as an OC, respectively.

Blood samples (300  $\mu$ L) were collected in green-top vacutainers (containing sodium heparin) via an in-dwelling cannula placed on the jugular vein before and 0.083, 0.17, 0.25, 0.5, 1, 1.5, 2, 3, 4, 6, 8, and 12 h after capsaicin administration. The blood samples were centrifuged at 3000g for 15 min at room temperature, and the plasma was transferred to a separate plasma tube. The separated plasmas were stored at  $-70$   $^{\circ}$ C until analysis. The concentration of capsaicin in unknown samples was quantified by comparing peak area ratios from the unknown samples to those from the calibration curve.

**2.5.2. PK Analysis.** A non-compartmental approach was used for PK data analysis. The PK parameters were determined using WinNonlin (version 2.1; Pharsight Corporation, Mountain View, CA). The area under the curve from time zero to time infinity ( $AUC_{inf}$ ) was obtained by extrapolation using elimination rate constants. The maximum plasma concentration ( $C_{max}$ ) and the time to reach  $C_{max}$  ( $T_{max}$ ) were determined directly from the individual drug concentration against the time curves. The terminal elimination rate constant ( $k_e$ ) was estimated by linear regression from the points describing the elimination phase on a log-linear plot. Half-life ( $t_{1/2}$ ) was calculated by  $0.693/k_e$ . Total clearance ( $Cl$ ) was calculated by  $dose/AUC_{inf}$ . The volume of distribution ( $Vd$ ) was calculated by  $Cl/k_e$ . The relative bioavailability of formulated nanoemulsions to the capsaicin control was calculated from dose-normalized  $AUC_{inf}$  values.<sup>17</sup>

relative bioavailability

$$= (AUC_{test} \text{ dose}_{reference}) / (AUC_{reference} \text{ dose}_{test})$$

**2.6. Statistical Analysis.** The PK variables of all dosage forms were compared with a one-way analysis of variation (ANOVA), which was followed by a posterior test with the use of the Bonferroni correction. A  $p$  value of less than 0.05 was considered significant.

### 3. RESULTS AND DISCUSSION

Figure 1 shows the well-resolved chromatographic peaks of capsaicin and IS at 1.6 and 1.1 min, respectively. The blank plasma after extraction consistently contains no significant interfering peaks. A linear response between the peak area ratio of capsaicin to IS and capsaicin plasma concentration ranging from 0.5 to 50 ng/mL was obtained ( $r^2 = 0.9999$ ). Six different capsaicin concentrations were used to establish the standard curve.

The limit of quantitation (LOQ) of capsaicin was determined as the sample concentration of capsaicin resulting in peak heights of 10 times the signal-to-noise (SN) ratio. The LOQ was found to be 0.5 ng/mL. On the basis of 3 times the peak height of SN, the limit of detection was calculated to be 0.1 ng/mL. The intra- and interday precisions of the methods were determined by the assay of five samples of drug-free plasma containing known concentrations of capsaicin. As described in Table 1, the intra- and interday RSDs (%) were within 12.3%, which was acceptable for all quality control samples, including the LOQ. The accuracy of capsaicin ranged between 88.8 and 105.4%. All of the batches met the quality control acceptance criteria.<sup>18</sup>



**Table 1. Intra- and Interday Precision and Accuracy of the Determination of Capsaicin in Plasma**

concentration (ng/mL)	precision (CV, %) <sup>a</sup>		accuracy (%)	
	intraday (n = 5)	interday (n = 5)	intraday (n = 5)	interday (n = 5)
0.5	12.21	9.87	91.23	105.42
1	3.59	6.75	95.59	99.12
5	6.63	8.50	90.64	93.31
10	4.12	2.21	98.39	101.22
25	8.20	5.89	102.61	100.55
50	1.68	9.15	88.79	90.84

<sup>a</sup>Coefficient of variance (CV, %) = standard deviation (SD)/mean × 100.

The actual particle sizes and  $\zeta$  potentials of capsaicin-loaded nanoemulsions were determined using a ternary-phase diagram of a three-component system of OC/Tween 80/water, which was described in our prior paper.<sup>15</sup> The basic characteristics of the formulated nanoemulsions are shown in Table 2. As suggested in our previous study,<sup>15</sup> as the Tween 80 concentration increased, the particle size decreased, possibly because smaller particle sizes would require more surfactant to cover because of the greater surface areas.

Figure 2 shows the mean plasma concentration–time profiles after administration of three sizes of capsaicin-loaded nanoemulsions fabricated with alginate polymers (AN50, AN100, and AN150) and capsaicin control at a dose of 10 mg/kg as an OC, and Table 3 reveals the PK parameters based on Figure 2. Among the two parameters indicating absorption rates,  $T_{max}$  was not different among groups, whereas  $C_{max}$  was significantly higher in nanoemulsion groups compared to the control group ( $p < 0.01$ ). The increased  $C_{max}$  without shortened  $T_{max}$  was possibly explained by the decreased elimination rate and unchanged absorption rate.

Dramatically decreased elimination rate constants of nanoemulsions, more than 30 times compared to the capsaicin control, led to approximately 20 times higher  $C_{max}$  values. However, the  $T_{max}$  values were not affected by the decreased  $k_e$ . This was possibly because capsaicin absorption rates did not significantly increase from nanoemulsions compared to the capsaicin control, and because elimination rates are usually negligible compared to absorption rates in time  $< T_{max}$ ,  $T_{max}$  would mostly be affected by absorption rates only. Because the polymeric membrane of the nanoemulsions can act as a barrier to release, the capsaicin release rate can be controlled and sustained. Because the rate of drug output significantly decreased, while the rate of drug input was not changed much, the  $T_{max}$  was not shortened.

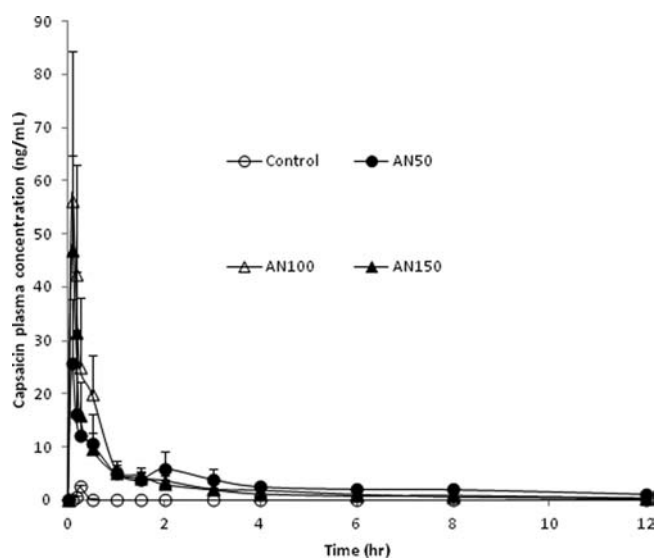


**Figure 2.** Time courses of plasma capsaicin concentrations following oral administration of various sizes of double-layer nanoemulsions fabricated with alginate (10 mg/kg as an OC) [mean  $\pm$  standard error (SE);  $n = 6$ ].

To improve bioavailability of lipophilic substances, such as capsaicin, a lot of technologies have been studied, including pro-drugs,<sup>19,20</sup> new salts,<sup>21</sup> crystal engineering,<sup>22</sup> lipid-based delivery systems,<sup>23–25</sup> cyclodextrin-based inclusion complexes,<sup>26</sup> nanosizing,<sup>27,28</sup> and hydroxypropyl methylcellulose acetate succinate-based spray-dried dispersions.<sup>29</sup> Among them, nanostructuring formulations effectively increase the solubility of lipophilic substances by increasing their surface area, resulting in higher absorption and bioavailability, because absorption is affected by solubility, which, in turn, can be increased by promoting solute–solvent interactions via bigger surface areas. However, the absorption rates in this study failed to show significant increases possibly because the use of natural biopolymers, such as alginate and chitosan, controlled the release of capsaicin, although the polymers could improve the problems of instability and degradation, which nanoemulsions possess.<sup>30</sup>

A statistically significant difference was found in  $AUC_{inf}$  among formulations ( $p < 0.01$ ), as shown in Table 3. In comparison to the control group, the relative bioavailability of nanoemulsions was up to 131.7. The higher  $AUC_{inf}$  values of nanoemulsions were attributable to the decreased  $k_e$  and  $Vd$ . It has been reported that the cutoff size of particles for renal clearance is about 5.5 nm.<sup>31</sup> Considering that the formulated

**Table 2. Basic Characteristics of Capsaicin-Loaded Nanoemulsions with Alginate, Chitosan, and Complexation with Alginate and Chitosan<sup>a</sup>**

OC/Tween 80	nanoemulsions	particle size (nm)	$\zeta$ potential (mV)	polydispersity index	encapsulation efficiency
1:0.5	AN50	53.4 $\pm$ 0.83	−42.1 $\pm$ 0.52	0.41 $\pm$ 0.04	98.24 $\pm$ 0.74
1:0.3	AN100	93.2 $\pm$ 0.71	−38.1 $\pm$ 0.14	0.44 $\pm$ 0.02	98.16 $\pm$ 0.52
1:0.2	AN150	149.3 $\pm$ 0.65	−36.7 $\pm$ 0.25	0.43 $\pm$ 0.05	98.32 $\pm$ 0.38
1:0.3	CN100	105.4 $\pm$ 0.22	36.5 $\pm$ 0.47	0.68 $\pm$ 0.04	98.01 $\pm$ 0.71
1:0.3	CAN100	106.7 $\pm$ 0.36	−25.4 $\pm$ 0.36	0.71 $\pm$ 0.03	95.07 $\pm$ 0.84

<sup>a</sup>Data are expressed as the mean  $\pm$  standard error of the mean (SEM) ( $n = 3$ ). OC, oleoresin capsicum; AN50, 50 nm double-layer nanoemulsions fabricated with alginate; AN100, 100 nm double-layer nanoemulsions fabricated with alginate; AN150, 150 nm double-layer nanoemulsions fabricated with alginate; CN100, 100 nm double-layer nanoemulsions fabricated with chitosan; and CAN100, 100 nm triple-layer nanoemulsions fabricated with chitosan/alginate.

**Table 3. Model-Independent PK Parameters of Capsaicin after Oral Administration of Various Sizes of Double-Layer Nanoemulsions Fabricated with Alginate<sup>a</sup>**

	capsaicin control	AN50	AN100	AN150
$T_{\max}$ (h)	0.25	0.48 ± 0.35	0.20 ± 0.08	0.55 ± 0.25
$C_{\max}$ ( $\mu\text{g/L}$ ) <sup>b</sup>	2.50 ± 0.47	48.55 ± 16.23 <sup>c</sup>	59.08 ± 27.14 <sup>c</sup>	60.62 ± 18.22 <sup>c</sup>
$t_{1/2}$ (h) <sup>b</sup>	0.11 ± 0.03	4.24 ± 0.95 <sup>c</sup>	3.82 ± 0.96 <sup>c</sup>	3.68 ± 0.84 <sup>c</sup>
$\text{AUC}_{\text{inf}}$ ( $\mu\text{g h L}^{-1}$ ) <sup>b</sup>	0.54 ± 0.07	71.14 ± 19.40 <sup>c</sup>	43.98 ± 9.30 <sup>c</sup>	38.75 ± 6.48 <sup>c</sup>
$k_e$ <sup>b</sup>	7.67 ± 1.71	0.25 ± 0.09 <sup>c</sup>	0.23 ± 0.07 <sup>c</sup>	0.23 ± 0.04 <sup>c</sup>
$Vd/F$ (L) <sup>d</sup>	807.95 ± 205.46	252.24 ± 64.98 <sup>c</sup>	402.50 ± 116.25 <sup>c</sup>	407.08 ± 120.03 <sup>c</sup>
$Cl/F$ (L/h) <sup>b</sup>	4894.85 ± 580.50	47.26 ± 10.78 <sup>c</sup>	79.58 ± 29.07 <sup>c</sup>	77.08 ± 14.19 <sup>c</sup>

<sup>a</sup>Data are expressed as the mean ± SE ( $n = 6$ ). The dose was 10 mg/kg as an OC. AN50, 50 nm double-layer nanoemulsions fabricated with alginate; AN100, 100 nm double-layer nanoemulsions fabricated with alginate; and AN150, 150 nm double-layer nanoemulsions fabricated with alginate.  $T_{\max}$ , time to  $C_{\max}$ ;  $C_{\max}$ , maximum concentration;  $t_{1/2}$ , half-life;  $\text{AUC}_{\text{inf}}$ , area under the curve from time zero to infinity;  $k_e$ , elimination rate constant;  $Vd$ , volume of distribution;  $F$ , bioavailability; and  $Cl$ , clearance. <sup>b</sup> $p < 0.01$  among the groups. <sup>c</sup> $p < 0.01$  versus the capsaicin control. <sup>d</sup> $p < 0.05$  among the groups.

**Table 4. Model-Independent PK Parameters of Capsaicin after Oral Administration of 100 nm Double- and Triple-Layer Nanoemulsions Fabricated with Alginate, Chitosan, and Alginate/Chitosan<sup>a</sup>**

	AN100	CN100	CAN100
$T_{\max}$ (h)	0.20 ± 0.08	0.15 ± 0.02	0.26 ± 0.18
$C_{\max}$ ( $\mu\text{g/L}$ )	59.08 ± 27.14	42.40 ± 9.90	48.95 ± 19.70
$t_{1/2}$ (h)	3.82 ± 0.96	6.18 ± 0.83	4.67 ± 1.15
$\text{AUC}_{\text{inf}}$ ( $\mu\text{g h L}^{-1}$ ) <sup>b</sup>	43.98 ± 9.30 <sup>c</sup>	41.51 ± 4.67 <sup>c</sup>	20.93 ± 2.79
$k_e$	0.23 ± 0.07	0.13 ± 0.02	0.34 ± 0.17
$Vd/F$ (L)	402.50 ± 116.25	589.26 ± 96.41	1113.78 ± 370.37
$Cl/F$ (L/h) <sup>b</sup>	79.58 ± 29.07 <sup>c</sup>	66.43 ± 9.82 <sup>c</sup>	136.34 ± 18.67

<sup>a</sup>Data are expressed as the mean ± SE ( $n = 6$ ). The dose was 10 mg/kg as an OC. AN100, 100 nm double-layer nanoemulsions fabricated with alginate; CN100, 100 nm double-layer nanoemulsions fabricated with chitosan; and CAN100, 100 nm triple-layer nanoemulsions fabricated with chitosan/alginate.  $T_{\max}$ , time to  $C_{\max}$ ;  $C_{\max}$ , maximum concentration;  $t_{1/2}$ , half-life;  $\text{AUC}_{\text{inf}}$ , area under the curve from time zero to infinity;  $k_e$ , elimination rate constant;  $Vd$ , volume of distribution;  $F$ , bioavailability; and  $Cl$ , clearance. <sup>b</sup> $p < 0.01$  among the groups. <sup>c</sup> $p < 0.05$  versus CAN100.

capsaicin-loaded nanoemulsions are much larger than the cutoff size, they could avoid renal excretion. Moreover, when encapsulated in nanoparticles, capsaicin could be protected from metabolizing enzymes in the liver.<sup>32</sup> Therefore, the  $k_e$  value of capsaicin encapsulated in the nanoparticles was thought to be lowered because of the reduced liver metabolism and renal clearance.

Nanoparticles are not able to diffuse through the capillary wall into the tissue because of their large sizes. The endothelial wall in the tissue has a limited pore size and, thus, blocks the delivery of nanoparticles. Therefore, the distribution of nanoparticles can be very low. Accordingly, in this study, the  $Vd$  values were much lower than that of the capsaicin control ( $p < 0.05$ ).

The  $\text{AUC}_{\text{inf}}$  decreased in a size-dependent manner; as particle sizes increased, the  $\text{AUC}_{\text{inf}}$  decreased. This was not caused by the elimination rate increase but by the distribution increase. As shown in Table 3, a markedly increased  $Vd$  was obtained with AN100 and AN150 compared to AN50. Because the  $k_e$  values were not different among the three nanoemulsions with alginate polymers, the low  $Vd$  of AN50 resulted in the significantly lowered  $Cl$  and increased  $\text{AUC}_{\text{inf}}$  compared to AN100 and AN150.

Nanosizes are known to be an important determinant of the nanoparticle distribution.<sup>33</sup> As mentioned above, normally, nanoparticles are not able to diffuse through the endothelial wall in the tissue because of their large sizes, thereby causing reduced distribution. However, the distribution of big nanosizes could rather increase instead of decrease compared to that of small nanosizes. It has been shown that nanoparticles with sizes bigger than 100 nm could be more vulnerable to mononuclear

phagocyte systems (MPS) residing in the tissues than those smaller than 100 nm, and for nanoparticles with sizes bigger than 100 nm, the clearance rate by the mononuclear phagocyte system increased with a size increase.<sup>32,34,35</sup> Another study revealed that that smaller vesicles (25/50 nm) resulted in lower liver uptake than bigger vesicles (200/300 nm), which could also be a factor affecting distributions of nanoemulsions.<sup>36</sup> Therefore, the higher  $Vd$  in AN100 and AN150 was thought to be due to higher clearance by MPS and liver uptake compared to AN50.

The effect of polymers used for the nanoconstruction was examined using alginate, chitosan, and a combination of alginate and chitosan (1:1), all 100 nm in size (Table 4). There was no significant difference in PK parameters between alginate and chitosan. However, in comparison to the double-layer nanoemulsions, the triple-layer nanoemulsion, which was prepared by complexation with chitosan and alginate, showed significantly increased  $Vd$ , resulting in the increased  $Cl$  and decreased  $\text{AUC}_{\text{inf}}$  (Figure 3). In the previous study,<sup>14</sup> the  $\zeta$  potential value, an indicator of the overall stability and physicochemical properties of nanoemulsions fabricated with the chitosan/alginate combination, was significantly lower than those of alginate and chitosan. This was explained because of the coexistence of anions from alginate and cations from chitosan by bonding with deposited electrical ions.<sup>14</sup> The relative instability of the chitosan/alginate combination was thought to reduce the preservation of drug activity, increasing clearance.

On the basis of the results, it was concluded that the dose of capsaicin loaded in nanoemulsions can be greatly reduced because the prepared nanoemulsions showed up to 131.7 times

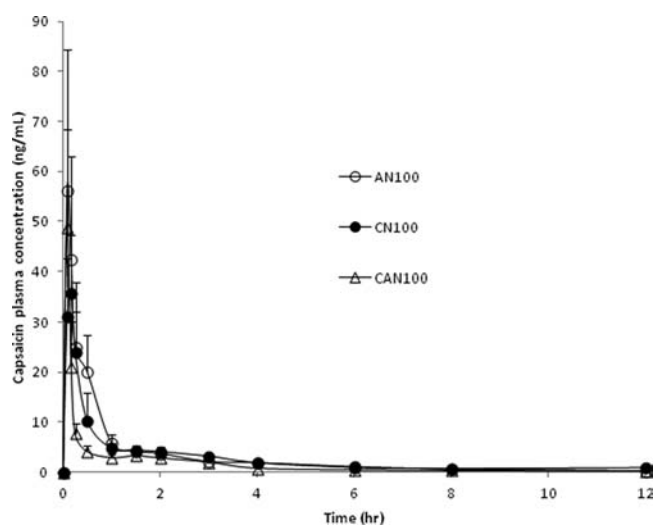


**Figure 3.** Time courses of plasma capsaicin concentrations following oral administration of 100 nm triple-layer nanoemulsions fabricated with chitosan/alginate (10 mg/kg as an OC) (mean  $\pm$  SE;  $n = 6$ ).

higher bioavailability with prolonged half-life and decreased distribution compared to the capsaicin control. This shows a great potential for commercialization into a dietary supplement with only small amounts of capsaicin-loaded nanoemulsions.

## AUTHOR INFORMATION

### Corresponding Author

\*Telephone: +82-2-3277-4376. Fax: +82-2-3277-2851. E-mail: hsgwak@ewha.ac.kr.

### Notes

The authors declare no competing financial interest.

## REFERENCES

- Reyes-Escogido, M. L.; Gonzalez-Mondragon, E. G.; Vazquez-Tzompantzi, E. Chemical and pharmacological aspects of capsaicin. *Molecules* **2011**, *16*, 1253–1270.
- Cortright, D. N.; Szallasi, A. Biochemical pharmacology of the vanilloid receptor TRPV1. *Eur. J. Biochem.* **2004**, *271*, 1814–1819.
- Tominaga, M.; Tominaga, T. Structure and function of TRPV1. *Pflugers Arch.* **2005**, *451*, 143–150.
- Bevan, S.; Szolcsanyi, J. Sensory neuron-specific actions of capsaicin: mechanisms and applications. *Trends Pharmacol. Sci.* **1990**, *11*, 330–333.
- Molina-Torres, J.; Garcia-Chavez, A.; Ramirez-Chavez, E. Antimicrobial properties of alkamides present in flavoring plants traditionally used in Mesoamerica: Affinin and capsaicin. *J. Ethnopharmacol.* **1999**, *64*, 241–248.
- Ghosh, A. K.; Basu, S. Fas-associated factor 1 is a negative regulator in capsaicin induced cancer cell apoptosis. *Cancer Lett.* **2010**, *287*, 142–149.
- Zhang, J.; Nagasaki, M.; Tanaka, Y.; Morikawa, S. Capsaicin inhibits growth of adult T-cell leukemia cells. *Leuk. Res.* **2003**, *27*, 275–283.
- Nishihara, K.; Nozawa, Y.; Nakano, M.; Ajioka, H.; Matsuura, N. Sensitizing effects of lafutidine on CGRP-containing afferent nerves in the rat stomach. *Br. J. Pharmacol.* **2002**, *135*, 1487–1494.
- Peng, J.; Li, Y. J. The vanilloid receptor TRPV1: role in cardiovascular and gastrointestinal protection. *Eur. J. Pharmacol.* **2010**, *627*, 1–7.
- Spemath, A.; Yaghmur, A.; Aserin, A.; Hoffman, R. E.; Garti, N. Food-grade nanoemulsions based on nonionic emulsifiers: media to enhance lycopene solubilization. *J. Agr. Food Chem.* **2002**, *50*, 6917–6922.
- Wang, L.; Li, X.; Zhang, G.; Dong, J.; Eastoe, J. Oil-in-water nanoemulsions for pesticide formations. *J. Colloid Interface Sci.* **2007**, *314*, 230–235.
- Kim, S.; Kim, J. C.; Sul, D.; Hwang, S. W.; Lee, S. H.; Kim, Y. H.; Tae, G.; Kim, J. Nanoparticle formulation for controlled release of capsaicin. *Nanosci. Nanotechnol.* **2011**, *11*, 4586–4591.
- Contri, R. V.; Kaiser, M.; Poletto, F. S.; Pohlmann, A. R.; Guterres, S. S. Simultaneous control of capsaicinoids release from polymeric nanocapsules. *J. Nanosci. Nanotechnol.* **2011**, *11*, 2398–2406.
- Choi, A.; Kim, C.; Cho, Y.; Hwang, J.; Kim, C. Characterization of capsaicin-loaded nanoemulsions stabilized with alginate and chitosan by self-assembly. *Food Bioprocess Technol.* **2011**, *4*, 1119–1126.
- Choi, A.; Kim, C.; Cho, Y.; Hwang, J.; Kim, J. Effects of surfactants on the formation and stability of capsaicin-loaded nanoemulsions. *Food Sci. Biotechnol.* **2009**, *18*, 1161–1172.
- Seo, S. B.; Toshio, K. Preparation of water soluble chitosan blends and their application to removal of heavy metal ions from wastewater. *Macromol. Res.* **2002**, *10*, 103–107.
- Eriksson, T.; Granérus, A. K.; Linde, A.; Carlsson, A. 'On-off' phenomenon in Parkinson's disease: relationship between dopa and other large neutral amino acids in plasma. *Neurology* **1998**, *38*, 1245–1248.
- Kamas, H. T.; Shiu, G.; Shah, V. P. Validation of bioanalytical methods. *Pharm. Res.* **1991**, *8*, 421–426.
- Fleisher, D.; Bong, R.; Stewart, B. H. Improved oral drug delivery: solubility limitations overcome by the use of prodrugs. *Adv. Drug Delivery Rev.* **1996**, *19*, 115–130.
- Stella, V. J.; Nti-Addae, K. W. Prodrug strategies to overcome poor water solubility. *Adv. Drug Delivery Rev.* **2007**, *59*, 677–694.
- Serajuddin, A. T. M. Salt formation to improve drug solubility. *Adv. Drug Delivery Rev.* **2007**, *59*, 603–616.
- Blagden, N.; de Matas, M.; Gavan, P. T.; York, P. Crystal engineering of active pharmaceutical ingredients to improve solubility and dissolution rates. *Adv. Drug Delivery Rev.* **2007**, *59*, 617–630.
- Humberstone, A. J.; Charman, W. N. Lipid-based vehicles for the oral delivery of poorly water soluble drugs. *Adv. Drug Delivery Rev.* **1997**, *25*, 103–128.
- Porter, C. J. H.; Pouton, C. W.; Cuine, J. F.; Charman, W. N. Enhancing intestinal drug solubilization using lipid-based delivery systems. *Adv. Drug Delivery Rev.* **2008**, *60*, 673–691.
- Tang, J.; Sun, J.; He, Z. Self-emulsifying drug delivery systems: strategy for improving oral delivery of poorly soluble drugs. *Curr. Drug Ther.* **2007**, *2*, 85–93.
- Brewster, M. E.; Loftsson, T. Cyclodextrins as pharmaceutical solubilizers. *Adv. Drug Delivery Rev.* **2007**, *59*, 645–666.
- Kesisoglou, F.; Panmai, S.; Wu, Y. Nanosizing-oral formulation development and biopharmaceutical evaluation. *Adv. Drug Delivery Rev.* **2007**, *59*, 631–644.
- Merisko-Liversidge, E.; Liversidge, G. G.; Cooper, E. R. Nanosizing: a formulation approach for poorly-water-soluble compounds. *Eur. J. Pharm. Sci.* **2003**, *18*, 113–120.
- Friesen, D. T.; Shanker, R.; Crew, M.; Smithy, D. T.; Curatolo, W. J.; Nightingale, J. A. S. Hydroxypropyl methylcellulose acetate succinate-based spray-dried dispersions: an overview. *Mol. Pharmaceutics* **2008**, *5*, 1003–1019.
- Weiss, J.; Takhistov, P.; McClements, J. Functional materials in food nanotechnology. *J. Food Sci.* **2006**, *71*, 107–116.
- Choi, H. S.; Liu, W.; Misra, P.; Tanaka, E.; Zimmer, J. P.; Ito, Ipe, B.; Bawendi, M. G.; Frangioni, J. V. Renal clearance of quantum dots. *At. Biotechnol* **2007**, *25*, 1165–1170.
- Li, S.; Huang, L. Pharmacokinetics and biodistribution of nanoparticles. *Mol. Pharmaceutics* **2008**, *5*, 496–504.
- De Jong, W. H.; Borm, P. J. A. Drug delivery and nanoparticles: applications and hazards. *Int. J. Nanomedicine* **2008**, *3*, 133–149.
- Senior, J.; Gregoriadis, G. Is half-life of circulating small unilamellar liposomes determined by changes in their permeability? *FEBS Lett.* **1982**, *145*, 109–114.

(35) Senior, J.; Crawley, J. C. W.; Fisher, D.; Tilcock, C.; Gregoriadis, G. Influence of surface hydrophobicity of liposomes on their interaction with plasma protein and clearance from the circulation: studies with poly (ethylene glycol)-coated vesicles. *Biochim. Biophys. Acta* **1991**, *1062*, 77–82.

(36) Seki, J.; Sonoke, S.; Saheki, A.; Fukui, H.; Sasaki, H.; Mayumi, T. A nanometer lipid emulsion, lipid nano-sphere (LNS), as a parenteral drug carrier for passive drug targeting. *Int. J. Pharm.* **2004**, *273*, 75–83.